Miscible Polyether/Poly(ether–acetal) Electrolyte Blends

Kevin W. Gao,

Department of Chemical and Biomolecular Engineering, University of California, Berkeley, Berkeley, California 94720, United States; Materials Sciences Division, Lawrence Berkeley National Laboratory, Berkeley, California 94720, United States; Joint Center for Energy Storage Research (JCESR), Argonne National Laboratory, Lemont, Illinois 60439, United States

Whitney S. Loo,

Department of Chemical and Biomolecular Engineering, University of California, Berkeley, Berkeley, California 94720, United States

Rachel L. Snyder,

Department of Chemistry and Chemical Biology, Cornell University, Ithaca, New York 14850, United States; Joint Center for Energy Storage Research (JCESR), Argonne National Laboratory, Lemont, Illinois 60439, United States

Brooks A. Abel,

Department of Chemistry and Chemical Biology, Cornell University, Ithaca, New York 14850, United States; Joint Center for Energy Storage Research (JCESR), Argonne National Laboratory, Lemont, Illinois 60439, United States

Youngwoo Choo,

Materials Sciences Division, Lawrence Berkeley National Laboratory, Berkeley, California 94720, United States; Joint Center for Energy Storage Research (JCESR), Argonne National Laboratory, Lemont, Illinois 60439, United States

Andrew Lee,

Department of Chemical and Biomolecular Engineering, NYU Tandon School of Engineering, New York University, Brooklyn, New York 11201, United States

Susana C. M. Teixeira,

NIST Center for Neutron Research, National Institute of Standards and Technology, Gaithersburg, Maryland 20899, United States; Department of Chemical and Biomolecular Engineering, University of Delaware, Newark, Delaware 19716, United States

Corresponding Authors: nbalsara@berkeley.edu; coates@cornell.edu.

Bruce A. Garetz,

Department of Chemical and Biomolecular Engineering, NYU Tandon School of Engineering, New York University, Brooklyn, New York 11201, United States

Geoffrey W. Coates,

Department of Chemistry and Chemical Biology, Cornell University, Ithaca, New York 14850, United States; Joint Center for Energy Storage Research (JCESR), Argonne National Laboratory, Lemont, Illinois 60439, United States

Nitash P. Balsara

Department of Chemical and Biomolecular Engineering, University of California, Berkeley, Berkeley, California 94720, United States; Materials Sciences Division, Lawrence Berkeley National Laboratory, Berkeley, California 94720, United States; Joint Center for Energy Storage Research (JCESR), Argonne National Laboratory, Lemont, Illinois 60439, United States

Abstract

This study shows that it is possible to obtain homogeneous mixtures of two chemically distinct polymers with a lithium salt for electrolytic applications. This approach is motivated by the success of using mixtures of organic solvents in modern lithium-ion batteries. The properties of mixtures of a polyether, poly(ethylene oxide) (PEO), a poly(ether–acetal), poly(1,3,6-trioxocane) (P(2EO-MO)), and lithium bis(trifluoromethanesulfonyl)imide (LiTFSI) salt were studied by small-angle neutron scattering (SANS) and electrochemical characterization in symmetric cells. The SANS data are used to determine the miscibility window and quantify the effect of added salt on the thermodynamic interactions between the polymers. In the absence of salt, PEO/P(2EO-MO) blends are homogeneous and characterized by attractive interactions, i.e., a negative Flory–Huggins interaction parameter, χ. The addition of small amounts of salt results in a positive effective Flory–Huggins interaction parameter, χ_{eff}, and macrophase separation. Surprisingly, miscible blends and negative χ_{eff} parameters are obtained when the salt concentration is increased beyond a critical value. The electrochemical properties of PEO/P(2EO-MO)/LiTFSI blends at a given salt concentration were close to those obtained in PEO/LiTFSI electrolytes at the same salt concentration. This suggests that in the presence of PEO the electrochemical properties exhibited by P(2EO-MO) chains are similar to those of PEO chains. This work opens the door to a new direction for creating new and improved polymer electrolytes either by combining existing polymers and salt or by synthesizing new polymers with the specific aim of including them in miscible polymer blend electrolytes.

Graphical Abstract

INTRODUCTION

There is considerable interest in replacing flammable organic solvents with nonvolatile polymers in rechargeable lithium batteries. It has long been recognized that high dielectric constant and low viscosity are necessary for rapid ion transport in liquid electrolytes. In the case of lithium-ion batteries designed to operate at room temperature, this is achieved by blending materials. Ethylene carbonate has a dielectric constant of 89.8 but is a solid at room temperature (mp = 36.4 °C) while dimethyl carbonate is a low-viscosity liquid (mp = 4.6 °C) but has a dielectric constant of 3.1.[1] Neither is a suitable solvent for electrolytic applications. However, a blend of ethylene carbonate and dimethyl carbonate is an excellent solvent for these applications and is a major component of lithium-ion battery electrolytes.

Translating the notion of liquid electrolyte mixtures to polymer electrolyte blends is nontrivial. While most low molar mass liquids are miscible with each other (e.g., polar molecules like ethanol are miscible in nonpolar liquids such as hexanes), finding pairs of miscible polymers is extremely rare.[2,3] Polymers with seemingly minor differences in monomer structure are entirely immiscible. For example, the solubility of polyethylene in polypropylene (both polymers have empirical formulas CH_2) is negligible.[4,5] The reason for this is well established: mixing is usually promoted by entropic considerations. The entropic gain of mixing polymers with long chains, however, is orders of magnitude smaller due to the connectivity of the monomers.

The purpose of this paper is to demonstrate that it is possible to create homogeneous mixtures of polymers with different polarities to create a new type of material for use in lithium batteries: miscible polymer blend electrolytes.

Our system of interest is a blend of a polyether, poly(ethylene oxide) (PEO), a poly(ether–acetal), poly-(1,3,6-trioxocane) (P(2EO-MO)), and lithium bis(trifluoromethanesulfonyl)imide (LiTFSI) salt (see Figure 1). PEO has been thoroughly studied as a potential electrolyte for lithium batteries due to its nonvolatility, electrochemical stability, and compatibility with lithium salts.[6–8] The ability of PEO to dissolve lithium salts is due to the presence of oxygen-containing ether linkages. The properties of P(2EO-MO)/LiTFSI electrolytes were reported in ref 9. We expect P(2EO-MO) to be more polar than PEO due to the increased concentration of ether and acetal oxygens. Ternary blends with polymer components of different polarities have been discussed as a means for improving ion transport in a recent theoretical paper by using a coarse-grained bead–spring model.[10]

In this work, we demonstrate that PEO is miscible with P(2EO-MO) in the neat, salt-free, state. We have also identified a range of salt concentrations over which PEO/P(2EO-MO)/LiTFSI blends remain miscible. We use the term *conventional polymer electrolytes* to refer to binary mixtures of a polymer and a salt such as PEO/LiTFSI or P(2EO-MO)/LiTFSI. We use the term *polymer blend electrolyte* to refer to ternary mixtures of two distinct polymers and a salt. The thermodynamic properties of PEO/P(2EO-MO)/LiTFSI were determined by small-angle neutron scattering (SANS) experiments. The SANS results are consistent with phase behavior inferences based on differential scanning calorimetry (DSC) experiments. Ion transport in the polymer blend electrolytes is compared with that obtained from conventional polymer electrolytes (PEO/LiTFSI and P(2EO-MO)/LiTFSI) by using both blocking and nonblocking electrodes.

MATERIALS AND METHODS

Synthesis of 1,3,6-Trioxocane, (2EO-MO).

Diethylene glycol (100 g, 0.942 mol), paraformaldehyde (37 g, 1.3 equiv), poly-(phosphoric acid) (4.0 g, 0.03 equiv), and heptane (160 mL) were combined in a 250 mL flask fitted with a Dean–Stark adapter and condenser. The reaction was stirred at 115 °C for 12 h, and water (~15 mL) was collected as the bottom layer in the trap. After the reaction mixture was cooled to room temperature, heptane was removed via rotary evaporation to give a cloudy, viscous solution. This oligomerized product was distilled at 150–180 °C under high vacuum into a receiving flask cooled in a dry ice/acetone bath. The crude mixture of diethylene glycol and 1,3,6-trioxocane was then fractionally distilled under high vacuum at 80 °C to give clear, colorless 1,3,6-trioxocane in 70% yield. The monomer was dried over CaH_2 for 3 days, distilled, and degassed via three freeze–pump–thaw cycles. Spectral data matched that previously reported in ref 9. ^{1}H NMR (500 MHz, $CDCl_3$): δ 4.57 (s, 2H), 3.50 (s, 8H) ppm. ^{13}C NMR (125 MHz, $CDCl_3$): δ 97.91, 72.58, 70.61 ppm. HRMS (DART-MS): *m/z* calculated for $C_5H_{10}O_3$ [H]$^+$ 119.0703; found 119.0703.

Synthesis of Poly(1,3,6-trioxocane), P(2EO-MO).

In a glovebox under a N_2 atmosphere, 1,3,6-trioxocane (6.0 g, 51 mmol) and CH_2Cl_2 (25.4 mL) were combined in a 100 mL flask equipped with a stir bar. Then, $BF_3 \cdot OEt_2$ (0.130 mL, 0.02 equiv) was added instantaneously, and the flask was sealed with a rubber septum. The reaction gelled after 30 min such that stirring ceased, and the solution gradually turned pink. After 1 h, the reaction was removed from the glovebox and quenched with a 1:1 mixture of acetonitrile:water (40 mL) to give a clear, colorless solution. The crude mixture was extracted with CH_2Cl_2 (30 mL × 3), dried with Na_2SO_4, filtered, and rotovapped until reaching a total volume of ~30 mL. The polymer was then precipitated into hexanes (400 mL), redissolved in CH_2Cl_2 (30 mL), and precipitated again into cold isopropanol (400 mL) to give a white solid. The polymer was dried under high vacuum overnight. Typical yields ranged from 50 to 60%, and ^{1}H and ^{13}C NMR analyses suggest that the polymerization proceeds with excellent regioregularity. Notably, polymerization is initiated by adventitious water in the reaction mixture. Furthermore, monomer conversion is highly dependent on monomer concentration and reaction temperature. Therefore, molar mass is difficult to control in this system, and variance was expected across multiple batches. Sample 1: M_n =

26.1 kg mol^{-1}, = 1.83. Sample 2: M_n = 16.1 kg mol^{-1}, = 1.76. Sample 3: M_n = 26.7 kg mol^{-1}, = 1.66. Sample 4: M_n = 55.2 kg mol^{-1}, = 1.97. T_g = −66 °C, T_m = 39 °C. Spectral data matched that previously reported in ref 9. ^{1}H NMR (500 MHz, CDCl$_3$): δ 4.74 (s, 2H), 3.69 (m, 8H) ppm. ^{13}C NMR (125 MHz, CDCl$_3$): δ 95.73, 70.60, 67.02 ppm.

Polymer Blend Electrolyte Preparation and Composition.

The molar masses, M_n, and dispersities, , of PEO (Polymer Source), deuterated PEO (dPEO) (Polymer Source), and P(2EO-MO) (synthesized as described above) used in this study are summarized in Table 1.

Electrolytes used for SANS experiments were made up of blends of dPEO, P(2EO-MO) (M_n = 26.7 or 16.0 kg mol^{-1}), and LiTFSI, while electrolytes for DSC and electrochemical experiments were made up of blends of PEO, P(2EO-MO) (M_n = 26.1 kg mol^{-1}), and LiTFSI (see Table 2). Electrochemical measurements were also performed on conventional polymer electrolytes of P(2EO-MO) (M_n = 55.2 kg mol^{-1}) with LiTFSI. All polymers were dried in a glovebox antechamber under vacuum at 90 °C for at least 24 h prior to use. LiTFSI was dried under vacuum at 120 °C for at least 72 h.

The polymer composition of the blends was 50/50 by weight. We denote component 1 as PEO and component 2 as P(2EO-MO). The volume fraction of each component, on a salt-free basis, is given by

$$\phi_1 = \frac{\frac{w_1}{\rho_1}}{\frac{w_1}{\rho_1} + \frac{w_2}{\rho_2}} \tag{1}$$

and

$$\phi_2 = 1 - \phi_1 \tag{2}$$

where w_i and ρ_i are the mass and density, respectively, of component i in the blend. The volume fractions are approximately equal (see Table 3). The volume fraction occupied by the polymer components in the blends containing LiTFSI is given by

$$\phi_{\text{polymer}} = \frac{\frac{w_1}{\rho_1} + \frac{w_2}{\rho_2}}{\frac{w_1}{\rho_1} + \frac{w_2}{\rho_2} + \frac{w_{\text{salt}}}{\rho_{\text{salt}}}} \tag{3}$$

where w_{salt} is the mass of LiTFSI in the blend and ρ_{salt} = 2.023 g cm^{-3}.[11] Volume changes of mixing are ignored in our analysis.

We assume that the salt is uniformly distributed in the blend. The salt concentration of the blends was quantified by the molar ratio of Li atoms in the salt to O atoms in the polymers (r = [Li]/[O]), calculated as follows:

$$r = \frac{\dfrac{w_{\text{salt}}}{M_{\text{salt}}}}{\dfrac{w_1}{M_{\text{EO}}} + \dfrac{3w_2}{M_{\text{2EO}-\text{MO}}}} \tag{4}$$

where M_{EO} is the monomer molar mass of PEO ($M_{\text{EO}} = 44.05$ g mol^{-1}), $M_{\text{2EO-MO}}$ is the monomer molar mass of P(2EO-MO) ($M_{\text{2EO-MO}} = 118.1$ g mol^{-1}), and M_{salt} is the molar mass of LiTFSI ($M_{\text{salt}} = 287.1$ g mol^{-1}). A factor of 3 was included as 2EO-MO contains three oxygen atoms, while EO contains one oxygen atom per monomer, as shown in Figure 1.

The volume fraction of PEO and the LiTFSI associated with PEO in the polymer blend electrolytes, f, is estimated via the following equation:

$$f = \frac{\dfrac{w_1 + \dfrac{rw_1 M_{\text{salt}}}{M_1}}{\rho_1}}{\dfrac{w_1 + \dfrac{rw_1 M_{\text{salt}}}{M_1}}{\rho_1} + \dfrac{w_2 + \dfrac{3rw_2 M_{\text{salt}}}{M_2}}{\rho_2}} \tag{5}$$

Equation 5 is based on the assumption that the value of r in the PEO-rich fluctuations is the same as that in the P(2EO-MO)-rich fluctuations.

Electrolyte r values ranged from 0 to 0.14. All electrolyte solutions in acetonitrile were transparent, indicating complete dispersion of all mixture components. The electrolytes were stirred on a hot plate at 80 °C until all of the acetonitrile had evaporated and then further dried in a glovebox antechamber under vacuum at 90 °C for 24 h to remove any residual solvent.

Density measurements for neat P(2EO-MO) at 90 °C were taken by measuring the mass of electrolyte within a known volume, following procedures described previously.[11] The average of three density measurements ($\rho_2 = 1.32 \pm 0.04$ g cm^{-3}) was used for subsequent calculations.

DSC Sample Preparation and Experiments.

Samples (~10 mg) were hermetically sealed in aluminum pans in an argon glovebox. DSC experiments were run with two heating and cooling cycles at a heating rate of 20 °C min^{-1} and a cooling rate of 5 °C min^{-1} using a Thermal Advantage Q200 calorimeter at the Molecular Foundry, Lawrence Berkeley National Lab. The temperature ranged from −80 to 120 °C. The glass transition temperature (T_g) values are obtained from analysis of the second heating run.

SANS Sample Preparation and Experiment.

Sample preparation for SANS experiments was conducted following procedures outlined previously.[12] The blends were made such that the volume fractions of each component were ~0.5 (see Table 3).

SANS experiments were conducted on the NG7SANS beamline at the National Institute of Standards and Technology Center for Neutron Research.[13] Measurements were performed with a neutron wavelength of 6 Å and up to three sample-to-detector distances (SDDs) of 13, 4, and 1 m. The shortest, 1 m distance, was used with a detector offset of 25 cm to extend the scattering angle (2θ) attainable. Overall, the three configurations allowed for access to a scattering wave-vector magnitude, $q = \frac{4\pi}{\lambda} \sin(\theta)$, ranging from 0.03 to 5.5 nm^{-1}. The neutron beam size was defined by a 9.5×10^{-3} m aperture. Data were collected at 10 °C increments between 60 and 110 °C. All measurements were reversible and repeatable upon either heating or cooling. Samples were equilibrated for at least 30 min at each temperature. A 9-position Peltier cooling/heating sample changer block was used to drive and maintain constant sample temperature. Samples of thickness of 1 mm were used. Data were reduced by using the software package for IGOR provided by the NIST Center for Neutron Research.[14] The total scattering intensity was corrected for detector sensitivity, background, and empty cell contributions as well as sample transmission and thickness.[14,15]

Electrochemical Sample Preparation and Experiments.

Electrochemical sample preparation and experiments were conducted following the procedures previously described,[16] using 508 μm thick silicone spacers and conducting the measurements at 90 °C.

RESULTS AND DISCUSSION

A commonly used method to determine polymer miscibility is the measurement of the glass transition temperature, T_g, via DSC. The existence of a single T_g is indicative of a miscible blend.[17] Figure 2a shows DSC curves for PEO/P(2EO-MO)/LiTFSI blends at $r = 0.04$ and 0.10. The $r = 0.04$ blend exhibits two glass transitions ($T_{g1} = -46$ °C, $T_{g2} = -38$ °C) which indicates the blend is phase separated. In contrast, the $r = 0.10$ blend exhibits a single glass transition ($T_g = -24$ °C), which indicates that the blend is composed of a single phase. The absence of a melting transition in the DSC data from the higher salt blend is consistent with numerous reports in the literature indicating that the addition of salt suppresses crystallization of PEO.[9,16,18,19] All of the thermodynamic and electrochemical data presented in this paper were obtained above the melting temperatures of the blends.

Figure 2b shows the complete set of glass transition temperatures for each polymer blend electrolyte and the corresponding conventional polymer electrolyte taken from ref 9. In the neat blend, the T_g values of PEO and P(2EO-MO) are too close to be distinguished by DSC. For r values between 0.02 and 0.06, the polymer blend electrolytes exhibit two T_g values, denoted by open squares, indicating immiscibility. However, from $r = 0.08$ to 0.14, the blend has a single T_g, indicating miscibility at these higher salt concentrations. The T_g for all systems generally increases with increasing salt concentration. The correlation between T_g and salt loading is attributed to the solvated ions inducing physical cross-linking of the polymer chains.[20]

The measured absolute SANS intensity, $I(q)$, as a function of the magnitude of the scattering vector, q, for the dPEO/P(2EO-MO)/LiTFSI blends at 90 °C is shown in Figure 3. Also

shown as a reference is a dPEO/PEO/LiTFSI blend with volume fraction $\phi_1 = 0.50$ and $r = 0.10$ at 90 °C. Distinct differences are apparent between the scattering profiles of dPEO/ P(2EO-MO)/LiTFSI blends with low salt concentrations (0.02 $\leq r \leq$ 0.06) and that of the neat blend ($r = 0$) and blends with high salt concentrations ($r \geq 0.08$). The blends with low salt concentration show a rapid rise in $I(q)$ at low q ($q < 0.1$ nm^{-1}), indicative of phase separation. The neat blend and high r-value blends have similar scattering profiles as that of the dPEO/PEO/LiTFSI sample. In the range $0.4 < q$ (nm^{-1}) < 2, $I(q)$ from these blends is approximately proportional to q^{-2} while $I(q)$ is a much weaker function of q for $q < 0.4$ nm^{-1}. These features are characteristic of scattering from a homogeneous binary polymer blend wherein the polymer chains obey random walk statistics.[21] The SANS results regarding polymer blend miscibility are consistent with the results obtained from DSC.

Analysis of SANS data begins with a thermodynamic model for the polymer blend electrolytes. We start with the thermodynamics of mixing in a two-component polymer blend in the absence of salt. The Gibbs free energy of mixing of a homogeneous mixture of two polymers can be described by the Flory–Huggins theory:

$$v\frac{\Delta G_m}{k_B T} = \frac{\phi_1 \ln \phi_1}{N_1} + \frac{\phi_2 \ln \phi_2}{N_2} + \chi\phi_1\phi_2 \tag{6}$$

where ΔG_m is the free energy of mixing per unit volume, k_B is the Boltzmann constant, T is the absolute temperature, ϕ_i is the volume fraction of component i, N_i is the number of repeat units in chain i, and χ is the Flory–Huggins interaction parameter which describes the thermodynamic incompatibility between component 1 and 2.[22,23] N_1, N_2 and χ are based on a reference volume, $v = 0.1$ nm^3. A miscible blend, one that is homogeneous down to the molecular level, requires both a negative Gibbs free energy of mixing ($\Delta G_m < 0$) and a positive second derivative ($\partial^2 \Delta G_m / \partial \phi_1^2 > 0$).[17] The critical Flory–Huggins interaction parameter value, χ_{crit}, is given by the following:

$$\chi_{crit} = \frac{1}{2}\left(\frac{1}{\sqrt{N_1}} + \frac{1}{\sqrt{N_2}}\right)^2 \tag{7}$$

Blends with $\chi < \chi_{crit}$ are predicted to be miscible, regardless of composition.

For salt-containing mixtures, we use a simple extension of eq 6:

$$v\frac{\Delta G_m}{k_B T} = \phi_{polymer}\left(\frac{\phi_1 \ln \phi_1}{N_1} + \frac{\phi_2 \ln \phi_2}{N_2} + \chi_{eff}\phi_1\phi_2\right) \tag{8}$$

where $\phi_{polymer}$ is the total polymer volume fraction and ϕ_i ($i = 1$ or 2) are the salt-free polymer volume fractions. The effect of added salt is captured mainly by an effective Flory–Huggins parameter, χ_{eff}, which depends on salt concentration. In the limit of $r \to 0$, $\phi_{polymer} \to 1$, eq 8 reduces to eq 6, and χ_{eff} reduces to the conventional χ parameter for polymer blends.

Following the analysis in ref 24, the absolute SANS intensity was corrected for the contributions from scattering of the deuterated chains as well as the contributions from the incoherent scattering to obtain the absolute coherent SANS intensity:

$$I_{coh}(q) = I(q) = f I_{dPEO / LiTFSI}(q) - I_{inc}(q) \tag{9}$$

where f is the estimated volume fraction of dPEO and LiTFSI in our polymer blend electrolytes ($f \approx 0.5$) and $I_{dPEO/LiTFSI}(q)$ is the scattering from dPEO/LiTFSI mixtures taken from ref 12. $I_{inc}(q)$ is the incoherent scattering background contribution to the intensities, determined by fitting $I(q)$ to the following expression:

$$I(q) = aP(q) + b \tag{10}$$

where $P(q)$ is a form factor given by the Debye function (see eq 14), a is a constant scaling factor, and b is a constant assumed to be equal to $I_{inc}(q)$.[14,15,25] Figure 4 shows the coherent SANS profiles, $I_{coh}(q)$, of the miscible blends at 90 °C.

The coherent scattering intensity for homogeneous PEO/P(2EO-MO)/LiTFSI blends is calculated by using the random phase approximation (RPA):

$$I_{coh}(q) = \phi_{polymer}(B_1 - B_2)^2 v \left(\frac{1}{S_{11}} + \frac{1}{S_{22}} + 2\chi_{eff} \right)^{-1} \tag{11}$$

In our analysis, component 1 is dPEO, component 2 is P(2EO-MO), $\phi_{polymer}$ is the volume fraction of both polymer components, dPEO and P(2EO-MO), B_i, is the coherent neutron scattering length density of component i given by $B_i = b_i / v_i$, v_i and b_i, are the molar monomer volumes and neutron scattering lengths of component i, respectively, and χ_{eff} is the effective Flory–Huggins interaction parameter between dPEO and P(2EO-MO) both with and without salt.[21,24,26–28] In the limit $q \to 0$, eq 11 is consistent with eq 8. The neutron scattering lengths of dPEO and P(2EO-MO) are 4.58×10^{-12} cm and 1.32×10^{-12} cm, respectively. The molar monomer volumes of dPEO and P(2EO-MO) were calculated in the absence of salt ($v_1 = 38.98$ cm^3 mol^{-1} and $v_2 = 89.47$ cm^3 mol^{-1} at 90 °C). We assume dPEO occupies the same molar volume as hydrogenous PEO. We thus obtain $\rho_1 = 1.23$ g cm^{-3} and $\rho_2 = 1.32$ g cm^{-3} at 90 °C. The temperature dependence of monomer volumes was applied to the contrast terms, and was determined by using the following equations: $\rho_1 = 1.23 - 7.31 \times 10^{-4}(T - 363)$ g cm^{-3} and $\rho_2 = 1.32 - 7.31 \times 10^{-4}(T - 363)$ g cm^{-3} where T is the temperature in Kelvin.[29] The thermal expansion coefficient of P(2EO-MO) has not been measured; it was assumed to be the same as that of PEO.

The structure factor, S_{ii}, is given by

$$S_{ii} = \phi_i N_i P_i(q) \tag{12}$$

where ϕ_i, is the volume fraction of polymer i on a salt-free basis. $I_{coh}(q)$ depends on three volume fractions: ϕ_1, ϕ_2, and $\phi_{polymer}$ (see eqs 11 and 12). For the blends covered in this study, these volume fractions are listed in Table 3.

N_i, is the number of repeat units in each polymer calculated by

$$N_i = \frac{M_i}{\rho_i N_{\mathrm{av}} v} \tag{13}$$

where N_{av} is Avogadro's number and M_i, and ρ_i, are the polymer molar masses (g mol^{-1}) and densities (g cm^{-3}) of component i, and

$$P_i(q) = 2\left[\frac{\exp(-x_i) - 1 + x_i}{x_i^2}\right] \tag{14}$$

with $x_i = q^2 R_{\mathrm{g},i}^2$. Both components are modeled as flexible Gaussian chains according to

$$R_{\mathrm{g},i}^2 = \frac{N_i l_i^2}{6} \tag{15}$$

where l_i, is the statistical segment length of each component. The statistical segment length of PEO is $l_1 = 0.58$ nm (based on a 0.1 nm^3 reference volume).[12] The statistical segment length of P(2EO-MO) has not been measured. In our calculations, we assume $l_1 = l_2 = l = 0.58a$ nm, where a is a fitting parameter that accounts for differences in the statistical segment length of PEO and P(2EO-MO) and distortions of chains (e.g., chain stretching) in the blends.

$I_{\mathrm{coh}}(q)$ values for the miscible blends were first fit to eq 11 with two adjustable parameters: a and χ_{eff}. For each blend, a was found to be essentially invariant with temperature so a was averaged across all temperatures and fixed. The parameter a is greater than 1 for all blends, likely due to the increased stiffness of P(2EO-MO) chains relative to that of the PEO chains. These values are given in Table 3. $I_{\mathrm{coh}}(q)$ was then fit to eq 11 with only χ_{eff} as a fitting parameter. Representative RPA fits of $I_{\mathrm{coh}}(q)$ for a dPEO/P(2EO-MO) blend with $r = 0.08$ are shown in Figure 5. χ_{eff} values of -4.67×10^{-3} and 7.64×10^{-4} are obtained from the profiles at 70 °C and 90 °C, respectively. At 110 °C, the blend is phase separated and cannot be analyzed by RPA. Note that χ_{eff} increases with increasing temperature.

Effective Flory–Huggins interaction parameters were extracted by fitting $I_{\mathrm{coh}}(q)$ to RPA for all miscible blends across a range of temperatures (60 $\leq$ T (°C) $\leq$ 110) for the high molar mass P(2EO-MO)-containing ($M_n = 26.7$ kg mol^{-1}) blends at $r = 0$, 0.08, 0.10, and 0.14 and the low molar mass P(2EO-MO)-containing ($M_n = 16.0$ kg mol^{-1}) blends at $r = 0$ and 0.10. The temperature dependence of χ_{eff} is given by

$$\chi_{\mathrm{eff}} = \frac{A}{T} + B \tag{16}$$

where A and B are empirically determined constants.[3,30] For each blend sample, χ_{eff} was linearly fit to inverse temperature using eq 16 to extract values for A and B. These values are summarized in Table 4.

All χ_{eff} parameters calculated in this study and their temperature and molar mass dependence are shown in Figure 6. Solid markers represent experimental measurements, and the solid lines are a fit to the data according to eq 16. The dashed line denotes χ_{crit}, which

was calculated from eqs 7 and 13 for blends comprising P(2EO-MO) of lower (16.0 kg mol^{-1}) and higher (26.7 kg mol^{-1}) molar masses. Figure 6a shows the temperature dependence of χ_{eff} in the higher molar mass P(2EO-MO)-containing blends. In the neat state, χ_{eff} is negative with a value of -3.07×10^{-3} at 60 °C and increases with increasing temperature (A = -5.401), increasing to a value of -9.67×10^{-4} at 110 °C. χ_{eff} is a more sensitive function of temperature in the salt-containing blends where $0.08 \leq r \leq 0.10$. For the $r = 0.08$ blend, χ_{eff} increases from -4.67×10^{-3} at 70 °C to 2.77×10^{-3} at 100 °C, and phase separation is observed experimentally at 110 °C (see Figure 5). At 110 °C, χ_{eff} predicted by extrapolating the data below 100 °C is larger than $\chi_{\text{crit}} = 5.06 \times 10^{-3}$, as expected. For $r = 0.10$, we see a similarly strong dependence with temperature, and χ_{eff} varies from -7.29×10^{-3} at 60 °C to -3.41×10^{-4} at 110 °C. The value of A is negative and B is positive for all miscible blends except at $r = 0.14$. At this concentration, A is positive and B is negative, and there is a very weak dependence on temperature.

Similarly, Figure 6b shows the temperature dependence of χ_{eff} in the lower molar mass P(2EO-MO)-containing blends. At the same salt concentration, the temperature dependences of χ_{eff} obtained from lower and higher molar mass P(2EO-MO) blends are similar. At $r = 0$, the difference in A and B values is less than 10%, while at $r = 0.10$, A is within 10% while the value of B differs by about 20% (see Table 4). The absolute value of χ_{eff} is greater in the lower molar mass P(2EO-MO)-containing blends than in the higher molar mass blends. χ_{eff} is always below $\chi_{\text{crit}} = 6.78 \times 10^{-3}$ for these lower molar mass blends.

In all cases where χ_{eff} is a sensitive function of temperature, R^2 values for the linear fits are greater than 0.98 (see Table 4). The R^2 value for the $r = 0.14$ blend is 0.344, which is expected as χ_{eff} is insensitive to temperature in this case.

Salt concentration is known to affect χ_{eff} in multicomponent polymer systems.[31,32] This effect has primarily been studied in phase-separated or microphase-separated systems, e.g., polystyrene and PEO.[33–42] In the dPEO/P(2EO-MO) (M_n = 26.7 kg mol^{-1}) blend, the addition of salt up to $r = 0.02$ induces phase separation, while sufficient salt concentrations ($r \geq 0.08$) render the mixture miscible again. The dependence of χ_{eff} on r is shown in Figure 7 for three temperatures (70 °C, 90 °C, and 110 °C). χ_{eff} is slightly negative in the neat blend, with similar values across the three temperatures. Addition of salt to $r = 0.02$ increases χ_{eff} above $\chi_{\text{crit}} = 5.06 \times 10^{-3}$. χ remains above this critical value at $r = 0.04$ and $r = 0.06$. Because the samples at $0.02 \leq r \leq 0.06$ were immiscible at all temperatures studied, no information about χ_{eff} is available besides a lower bound, as indicated in Figure 7. At 90 °C and 110 °C, χ_{eff} decreases with increasing r for $r \geq 0.08$. The data in Figure 7 suggest that χ_{eff} goes through a maximum at a value of r between 0.02 and 0.08 at 90 °C and 110 °C. At 70 °C, χ_{eff} is a nonmonotonic function of r for $r \geq 0.08$. At this temperature, χ_{eff} exhibits both a maximum and a minimum with respect to r.

We now discuss the ion transport properties of the higher molar mass polymer blend electrolytes. For reference, we also include ion transport properties of conventional PEO/LiTFSI (M_n = 35.0 kg mol^{-1}) and P(2EO-MO)/LiTFSI (M_n = 55.2 kg mol^{-1}) electrolytes.[43] The ionic conductivity of the PEO/P(2EO-MO)/LiTFSI blend as a function of r is shown in Figure 8a. The conductivity increases with increasing r due to the higher concentration of

charge carrying species. To a good approximation, the conductivity of the blend matches that of PEO/LiTFSI at all values of r.

The salt diffusion coefficient, D, of the blend shown in Figure 8b is similar to that of the conventional P(2EO-MO)/LiTFSI polymer electrolyte system for r 0.02 but is nearly equal to that of PEO/LiTFSI for higher r. The dependence of the current fraction, ρ_+, of the polymer blend on r, plotted in Figure 8c, matches that of PEO/LiTFSI at all salt concentrations.[44]

One measure of the efficacy of an electrolyte is the product of the ionic conductivity and current fraction. This measure gives a metric for sustaining steady currents in battery applications at low current densities. The efficacies of all three electrolyte systems are similar, as shown in Figure 8d.

The immiscible blends obtained in the regime 0.01 r 0.06 undoubtedly contain macroscopic PEO-rich and P(2EO-MO)-rich domains. However, we expect a considerable concentration of P(2EO-MO) in the PEO-rich domains, and vice versa. The fact that the ion transport data (see Figure 8) obtained from immiscible blends do not differ significantly from that of miscible blends may be attributed to this effect. A more thorough investigation into the impact of miscibility on ion transport is warranted but is beyond the scope of this study.

We were curious whether ion transport behavior in miscible polymer blend electrolytes can be predicted based on the known properties of conventional polymer electrolytes. It is well-established that ionic conductivity in polymers depends on the relative segmental motion of the polymer backbone, which can be gauged by the T_g value.[9,19,45,46] The T_g values of the miscible polymer blend electrolytes (PEO/P(2EO-MO)/LiTFSI) were consistently between the T_g values of the PEO/LiTFSI and P(2EO-MO)/LiTFSI electrolytes (see Figure 2b). However, conductivity measurements indicate that PEO, the component with the lower T_g, dominates conductivity. At most salt concentrations, this general behavior also applies to the measured current fractions and salt diffusion coefficients (see Figures 8b and 8c). These observations do not indicate that only PEO chains contribute to conductivity; if this were the case, then the conductivity of the 50/50 polymer blend electrolytes would be half that of PEO/LiTFSI. The data in Figures 2b, 8b, and 8c suggest that the P(2EO-MO) chains in the miscible polymer blend electrolytes behave as if they were PEO. It is evident that ion transport in miscible polymer blend electrolytes differs qualitatively from that in conventional polymer electrolytes.

We conclude this section by reviewing previous studies of ion transport in polymer blends. It is important to distinguish between oligomers and polymers: PEO analogues such as tetraethylene glycol dimethyl ether (tetraglyme), a short chain molecule comprising four ethylene oxide units, are commonly used as solvents for electrolytic applications.[47–49] The ionic conductivity of PEO/LiTFSI mixtures is independent of chain length when the molar mass of the PEO chains exceeds 2 kg mol^{-1}.[50] The entanglement molar mass of PEO is also reported to be 2 kg mol^{-1}.[51] This value (2 kg mol^{-1}) serves as an approximate marker to distinguish between oligomers and polymers in the context of electrolytes. There have been

a few reports of mixtures of polymers, salts, and a third component.[52–61] Tsuchida et al. studied mixtures of PEO, poly(methyl methacrylate) (PMMA), and lithium perchlorate (LiClO$_4$); however, the molar masses of examined PEO ranged from 0.7 to 2 kg mol^{-1}.[52] While the miscibility of PEO and PMMA is well-established in the absence of salt,[62] the effect of added salt on miscibility is not yet known. Abraham et al. blended PEO and poly[bis((methoxyethoxy)ethoxy) phosphazene] (MEEP) with different lithium salts.[53] The molar mass of MEEP was not reported. Interestingly, the blends exhibited two exothermic melting transitions: one similar to that of pure PEO in the vicinity of 55 °C and an additional peak at 140 °C, in spite of the fact that MEEP is amorphous. This suggests the presence of two phases in the PEO/MEEP electrolytes. Li et al. prepared blends of PEO, poly(2-vinylpyridine) (P2VP), and LiClO$_4$. While PEO and P2VP are miscible in the absence of salt,[63] the possibility of salt-induced phase separation was not addressed. Kim et al. report both conductivity and current fraction in mixtures of PEO, poly(oligo[oxyethylene]oxysebacoyl), and LiClO$_4$.[57] This is one of the few studies on electrochemical properties in polymer blends that go beyond conductivity; however, miscibility of the polymers in the presence of salt was not established. Rocco et al. studied mixtures of PEO, poly(methyl vinyl ether–maleic acid), and LiClO$_4$ as well as PEO, poly(bisphenol A-*co*-epichlorohydrin), poly(vinyl ethyl ether), and LiClO$_4$ blends for use as electrolytes.[59,60] Inferences regarding miscibility were mainly made on the basis of DSC. In contrast to all previous studies,[52–61] this paper definitively demonstrates the miscibility of a polymer blend electrolyte system by using a rigorous approach based on SANS, wherein concentration fluctuations on the nanometer length scale are quantified. Unlike previous studies,[52–61] this work compares the characteristics of the PEO/P(2EO-MO)/LiTFSI polymer blend electrolyte system to that of its constituent polymer electrolytes (PEO/LiTFSI and P(2EO-MO)/LiTFSI).

CONCLUSION

This study demonstrates that it is possible to create homogeneous mixtures of chemically distinct polymers and a lithium salt for use in lithium batteries. This demonstration is nontrivial because polymers rarely mix with each other. Blending polymers for electrolytic applications is advantageous because of the ease of preparation and control of physical properties by simple changes in composition or chain lengths of the components. This initial study, based on PEO/P(2EO-MO)/LiTFSI, can serve as a template for future work aimed at optimizing ion transport in polymer electrolytes in a manner that mirrors the development of mixtures of organic solvents used in current day lithium ion batteries. The thermodynamic properties of PEO/P(2EO-MO)/LiTFSI blends, determined by SANS, are surprisingly complex. This initial study is restricted to blends with roughly equal volume fractions of PEO and P(2EO-MO). Neat PEO/P(2EO-MO) blends exhibit a negative Flory–Huggins interaction parameter across the accessible temperature window. If we assume that the phase behavior of PEO/P(2EO-MO)/LiTFSI blends can be approximated by Flory–Huggins theory for binary blends of homopolymers with an effective interaction parameter that accounts for the presence of salt, it would imply that these blends would be miscible irrespective of blend composition and chain lengths of the components. Adding a small amount of LiTFSI (0.02 r 0.06) renders the PEO/P(2EO-MO) blends immiscible; blends containing either 26.7 or

16.0 kg mol^{-1} P(2EO-MO) were immiscible. Increasing the salt concentration to $r > 0.08$ results in negative effective Flory–Huggins interaction parameters across the accessible temperature window, implying miscibility irrespective of blend composition and chain lengths of the components.

Ion transport in the blends was characterized by measuring the ionic conductivity, salt diffusion coefficient, and current fraction. Surprisingly, the values of these parameters in blends at a given salt concentration, r, were close to those obtained in conventional PEO/LiTFSI electrolytes at the same value of r. In other words, the blends that we have characterized thus far do not exhibit superior ion transport properties. However, a wide variety of ether- and carbonate-containing polymers have been synthesized for electrolytic applications.[64–67] This work opens the door to a new direction for creating new and improved polymer electrolytes either by combining existing polymers with salt or by synthesizing new polymers with the specific aim of including them in miscible polymer blend electrolytes.

Supplementary Material

Refer to Web version on PubMed Central for supplementary material.

ACKNOWLEDGMENTS

LIST OF SYMBOLS

PEO	poly(ethylene oxide)
P(2EO-MO)	poly(1,3,6-trioxocane)
LiTFSI	lithium bis(trifluoromethanesulfonyl)imide
SANS	small-angle neutron scattering
DSC	differential scanning calorimetry
2EO-MO	1,3,6-trioxocane
M_n	number-average molar mass (kg mol^{-1})
	dispersity

dPEO	deuterated poly(ethylene oxide)
ϕ_i	volume fraction of component i
$\phi_{polymer}$	volume fraction of polymer components in a blend containing LiTFSI
w_i	weight of component i (g)
w_{salt}	weight of LiTFSI salt (g)
ρ_i	density of component i (g cm^{-3})
ρ_{salt}	density of LiTFSI salt (g cm^{-3})
r	molar ratio of lithium to oxygen atoms
M_{EO}	monomer molar mass of PEO (g mol^{-1})
M_{2EO-MO}	monomer molar mass of P(2EO-MO) (g mol^{-1})
M_{salt}	molar mass of LiTFSI salt (g mol^{-1})
f	volume fraction of PEO and LiTFSI associated with PEO
T_g	glass transition temperature
SDD	sample-to-detector distance
θ	scattering angle
q	magnitude of the scattering vector (nm^{-1})
λ	wavelength (nm)
q	magnitude of the scattering vector (nm^{-1})
$I(q)$	measured absolute SANS intensity (cm^{-1})
G_m	free energy of mixing per unit volume (J m^{-3})
k_B	Boltzmann constant (m^2 kg s^{-2} K^{-1})
v	reference volume (nm^3)
T	absolute temperature (K)
N_i	number of repeat units per chain
χ	Flory–Huggins interaction parameter
χ_{crit}	critical Flory–Huggins interaction parameter
χ_{eff}	effective Flory–Huggins interaction parameter
$I_{coh}(q)$	coherent scattering intensity (cm^{-1})

$I_{\mathbf{dPEO/LiTFSI}}(q)$	SANS intensity from dPEO/LiTFSI mixtures (cm^{-1})
$I_{\mathbf{inc}}(q)$	incoherent scattering intensity (cm^{-1})
$P_i(q)$	form factor
B_i	neutron scattering length density of component i (cm^{-2} mol^{-1})
b_i	neutron scattering length of component i (cm mol^{-1})
v_i	monomer molar volume of component i (cm^3 mol^{-1})
S_{ii}	structure factor
M_i	molar mass of component i (g mol^{-1})
$R_{\mathbf{g},i}$	radius of gyration (cm)
l_i	statistical segment length of component i (nm)
a	RPA fitting parameter accounting for chain distortion
A, B	empirical constants for fitting χ
R^2	coefficient of determination
κ	ionic conductivity (S cm^{-1})
D	salt diffusion coefficient (cm^2 s^{-1})
ρ_+	current fraction
$\kappa\rho_+$	efficacy (S cm^{-1})
PMMA	poly(methyl methacrylate)
LiClO$_4$	lithium perchlorate
MEEP	poly[bis((methoxyethoxy)ethoxy)-phosphazene]
P2VP	poly(2-vinylpyridine)

REFERENCES

(1). Xu K Nonaqueous Liquid Electrolytes for Lithium-Based Rechargeable Batteries. Chem. Rev 2004, 104, 4303–4417. [PubMed: 15669157]

(2). Flory PJ Principles of Polymer Chemistry; Cornell University Press: Ithaca, NY, 1953.

(3). Knychała P; Timachova K; Banaszak M; Balsara NP 50th Anniversary Perspective: Phase Behavior of Polymer Solutions and Blends. Macromolecules 2017, 50 (8), 3051–3065.

(4). Lohse DJ The Melt Compatibility of Blends of Polypropylene and Ethylene-propylene Copolymers. Polym. Eng. Sci 1986, 26 (21), 1500–1509.

(5). Kwag H; Rana D; Cho K; Rhee J; Woo T; Lee BH; Choe S Binary Blends of Metallocene Polyethylene with Conventional Polyolefins: Rheological and Morphological Properties. Polym. Eng. Sci 2000, 40 (7), 1672–1681.

(6). Fenton DE; Parker JM; Wright PV Complexes of Alkali Metal Ions with Poly(Ethylene Oxide). Polymer 1973, 14 (11), 589.

(7). Armand M Polymer Solid Electrolytes - an Overview. Solid State Ionics 1983, 9–10, 745–754.

(8). Xue Z; He D; Xie X Poly(Ethylene Oxide)-Based Electrolytes for Lithium-Ion Batteries. J. Mater. Chem. A 2015, 3 (38), 19218–19253.

(9). Zheng Q; Pesko DM; Savoie BM; Timachova K; Hasan AL; Smith MC; Miller TF; Coates GW; Balsara NP Optimizing Ion Transport in Polyether-Based Electrolytes for Lithium Batteries. Macromolecules 2018, 51 (8), 2847–2858.

(10). Wheatle BK; Lynd NA; Ganesan V Effect of Host Incompatibility and Polarity Contrast on Ion Transport in Ternary Polymer-Polymer-Salt Blend Electrolytes. Macromolecules 2020, 53 (3), 875–884.

(11). Pesko DM; Timachova K; Bhattacharya R; Smith MC; Villaluenga I; Newman J; Balsara NP Negative Transference Numbers in Poly(Ethylene Oxide)-Based Electrolytes. J. Electrochem. Soc 2017, 164 (11), E3569–E3575.

(12). Loo WS; Mongcopa KI; Gribble DA; Faraone AA; Balsara NP Investigating the Effect of Added Salt on the Chain Dimensions of Poly(Ethylene Oxide) through Small-Angle Neutron Scattering. Macromolecules 2019, 52 (22), 8724–8732.

(13). Glinka CJ; Barker JG; Hammouda B; Krueger S; Moyer JJ; Orts WJ The 30 m Small-Angle Neutron Scattering Instruments at the National Institute of Standards and Technology. J. Appl. Crystallogr 1998, 31 (3), 430–445.

(14). Kline SR Reduction and Analysis of SANS and USANS Data Using IGOR Pro. J. Appl. Crystallogr 2006, 39 (6), 895–900.

(15). Kline S SANS Data Reduction Tutorial; NIST Center for Neutron Research: 2001.

(16). Gao KW; Jiang X; Hoffman ZJ; Sethi GK; Chakraborty S; Villaluenga I; Balsara NP Optimizing the Monomer Structure of Polyhedral Oligomeric Silsesquioxane for Ion Transport in Hybrid Organic-Inorganic Block Copolymers. J. Polym. Sci 2020, 58 (2), 363–371.

(17). Utracki LA; Wilkie CA Polymer Blends Handbook, 2nd ed.; Springer: New York, 2014.

(18). Vallée A; Besner S; Prud'Homme J Comparative Study of Poly(Ethylene Oxide) Electrolytes Made with $LiN(CF_3SO_2)_2$, $LICF_3SO_3$ and $LiClO_4$: Thermal Properties and Conductivity Behaviour. Electrochim. Acta 1992, 37 (9), 1579–1583.

(19). Lascaud S; Perrier M; Vallée A; Besner S; Prud'homme J; Armand M Phase Diagrams and Conductivity Behavior of Poly(Ethylene Oxide)-Molten Salt Rubbery Electrolytes. Macromolecules 1994, 27 (25), 7469–7477.

(20). Le Nest JF; Gandini A; Cheradame H; Cohen-Addad JP Influence of $LiClO_4$ on the Properties of Polyether Networks: Specific Volume and Glass Transition Temperature. Macromolecules 1988, 21 (4), 1117–1120.

(21). de Gennes PG Scaling Concepts in Polymer Chemistry; Cornell University Press: Ithaca, NY, 1979.

(22). Flory PJ Thermodynamics of High Polymer Solutions. J. Chem. Phys 1942, 10 (1), 51–61.

(23). Huggins ML Some Properties of Solutions of Long-Chain Compounds. J. Phys. Chem 1942, 46 (1), 151–158.

(24). Balsara NP; Fetters LJ; Hadjichristidis N; Lohse DJ; Han CC; Graessley WW; Krishnamoorti R Thermodynamic Interactions in Model Polyolefin Blends Obtained by Small-Angle Neutron Scattering. Macromolecules 1992, 25 (23), 6137–6147.

(25). Dubner WS; Schultz JM; Wignall GD Estimation of Incoherent Backgrounds in SANS Studies of Polymers. J. Appl. Crystallogr 1990, 23 (6), 469–475.

(26). de Gennes PG Theory of X-Ray Scattering by Liquid Macromolecules with Heavy Atom Labels. J. Phys. (Paris) 1970, 31 (2–3), 235–238.

(27). Hammouda B Random Phase Approximation for Compressible Polymer Blends. J. Non-Cryst. Solids 1994, 172–174, 927–931.

(28). Qiu J; Mongcopa KI; Han R; López-Barrón CR; Robertson ML; Krishnamoorti R Thermodynamic Interactions in a Model Polydiene/Polyolefin Blend Based on 1,2-Polybutadiene. Macromolecules 2018, 51 (8), 3107–3115.

(29). Mark JE Physical Properties of Polymers Handbook, 2nd ed.; Springer: New York, 2007.

(30). Bates FS; Fredrickson GH Block Copolymer Thermodynamics: Theory And Experiment. Annu. Rev. Phys. Chem 1990, 41 (1), 525–557. [PubMed: 20462355]

(31). Wang ZG Effects of Ion Solvation on the Miscibility of Binary Polymer Blends. J. Phys. Chem. B 2008, 112 (50), 16205–16213. [PubMed: 19368023]

(32). Nakamura I; Balsara NP; Wang ZG Thermodynamics of Ion-Containing Polymer Blends and Block Copolymers. Phys. Rev. Lett 2011, 107 (19), 1–5.

(33). Young WS; Epps TH Salt Doping in PEO-Containing Block Copolymers: Counterion and Concentration Effects. Macromolecules 2009, 42 (7), 2672–2678.

(34). Naidu S; Ahn H; Gong J; Kim B; Ryu DY Phase Behavior and Ionic Conductivity of Lithium Perchlorate-Doped Polystyrene-b-Poly(2-Vinylpyridine) Copolymer. Macromolecules 2011, 44 (15), 6085–6093.

(35). Huang J; Tong ZZ; Zhou B; Xu JT; Fan ZQ Salt-Induced Microphase Separation in Poly(ε-Caprolactone)-b-Poly(Ethylene Oxide) Block Copolymer. Polymer 2013, 54 (12), 3098–3106.

(36). Teran AA; Balsara NP Thermodynamics of Block Copolymers with and without Salt. J. Phys. Chem. B 2014, 118 (1), 4–17. [PubMed: 24229067]

(37). Irwin MT; Hickey RJ; Xie S; So S; Bates FS; Lodge TP Structure-Conductivity Relationships in Ordered and Disordered Salt-Doped Diblock Copolymer/Homopolymer Blends. Macromolecules 2016, 49 (18), 6928–6939.

(38). Xie S; Lodge TP Phase Behavior of Binary Polymer Blends Doped with Salt. Macromolecules 2018, 51, 266–274.

(39). Hou KJ; Qin J Solvation and Entropic Regimes in Ion-Containing Block Copolymers. Macromolecules 2018, 51, 7463–7475.

(40). Loo WS; Jiang X; Maslyn JA; Oh HJ; Zhu C; Downing KH; Balsara NP Reentrant Phase Behavior and Coexistence in Asymmetric Block Copolymer Electrolytes. Soft Matter 2018, 14 (15), 2789–2795. [PubMed: 29513329]

(41). Loo WS; Balsara NP Organizing Thermodynamic Data Obtained from Multicomponent Polymer Electrolytes: Salt-Containing Polymer Blends and Block Copolymers. J. Polym. Sci., Part B: Polym. Phys. 2019, 57 (18), 1177–1187.

(42). Morris MA; Sung SH; Ketkar PM; Dura JA; Nieuwendaal RC; Epps TH Enhanced Conductivity via Homopolymer-Rich Pathways in Block Polymer-Blended Electrolytes. Macromolecules 2019, 52 (24), 9682–9692.

(43). Gribble DA; Frenck L; Shah DB; Maslyn JA; Loo WS; Mongcopa KIS; Pesko DM; Balsara NP Comparing Experimental Measurements of Limiting Current in Polymer Electrolytes with Theoretical Predictions. J. Electrochem. Soc 2019, 166 (14), A3228–A3234.

(44). Galluzzo MD; Maslyn JA; Shah DB; Balsara NP Ohm's Law for Ion Conduction in Lithium and beyond-Lithium Battery Electrolytes. J. Chem. Phys 2019, 151 (2), 020901. [PubMed: 31301729]

(45). Ratner MA; Johansson P; Shriver DF P Olymer Electrolytes: Ionic Transport Mechanisms and Relaxation Coupling. MRS Bull. 2000, 25, 31–37.

(46). Borodin O; Smith GD Mechanism of Ion Transport in Amorphous Poly(Ethylene Oxide)/LiTFSI from Molecular Dynamics Simulations. Macromolecules 2006, 39, 1620–1629.

(47). Jung H-G; Hassoun J; Park J-B; Sun Y-K; Scrosati B An Improved High-Performance Lithium-Air Battery. Nat. Chem 2012, 4, 579–585. [PubMed: 22717445]

(48). Nasybulin E; Xu W; Engelhard MH; Nie Z; Burton SD; Cosimbescu L; Gross ME; Zhang J Effects of Electrolyte Salts on the Performance Li-O2 Batteries. J. Phys. Chem. C 2013, 117, 2635–2645.

(49). Jache B; Binder JO; Abe T; Adelhelm P A Comparative Study on the Impact of Different Glymes and Their Derivatives as Electrolyte Solvents for Graphite Co-Intercalation Electrodes in Lithium-Ion and Sodium-Ion Batteries. Phys. Chem. Chem. Phys 2016, 18, 14299–14316. [PubMed: 27165175]

(50). Teran AA; Tang MH; Mullin SA; Balsara NP Effect of Molecular Weight on Conductivity of Polymer Electrolytes. Solid State Ionics 2011, 203, 18–21.

(51). Fetters LJ; Lohse DJ; Milner ST; Graessley WW Packing Length Influence in Linear Polymer Melts on the Entanglement, Critical, and Reptation Molecular Weights. Macromolecules 1999, 32, 6847–6851.

(52). Tsuchida E; Ohno H; Tsunemi K; Kobayashi N Lithium Ionic Conduction in Poly(Methacrylic Acid)-Poly(Ethylene Oxide) Complex Containing Lithium Perchlorate. Solid State Ionics 1983, 11, 227–233.

(53). Abraham KM; Alamgir M; Reynolds RK Polyphosphazene-Poly(Olefin Oxide) Mixed Polymer Electrolytes. J. Electrochem. Soc 1989, 136 (12), 3576–3582.

(54). Orihara K; Yonekura H Nonlinear Effects on the Ionic Conductivity of Poly(Ethylene Oxide)/ Lithium Perchlorate Complexes Caused by the Blending of Poly(Vinyl Acetate). J. Macromol Sci. Chem. 1990, 27, 1217–1223.

(55). Li J; Mintz EA; Khan IM Poly(Ethylene Oxide)/(Poly(2-Vinylpyridine)/Lithium Perchlorate Blends. New Materials for Solid Polymer Electrolytes. Chem. Mater 1992, 4 (6), 1131–1134.

(56). Acosta JL; Morales E Structural, Morphological and Electrical Characterization of Polymer Electrolytes Based on PEO/PPO Blends. Solid State Ionics 1996, 85, 85–90.

(57). Kim D; Park J; Rhee H Conductivity and Thermal Studies of Solid Polymer Electrolytes Prepared by Blending Poly(Ethylene Oxide), Poly(Oligo[Oxyethylene]Oxysebacoyl) and Lithium Perchlorate. Solid State Ionics 1996, 83, 49–56.

(58). Jacob MME; Prabaharan SRS; Radhakrishna S Effect of PEO Addition on the Electrolytic and Thermal Properties of PVDF-LiClO4 Polymer Electrolytes. Solid State Ionics 1997, 104, 267–276.

(59). Rocco AM; da Fonseca CP; Pereira RP A Polymeric Solid Electrolyte Based on a Binary Blend of Poly(Ethylene Oxide), Poly(Methyl Vinyl Ether-Maleic Acid) and LiClO4. Polymer 2002, 43 (13), 3601–3609.

(60). Rocco AM; de Assis Carias A; Pereira RP Polymer Electrolytes Based on a Ternary Miscible Blend of Poly(Ethylene Oxide), Poly(Bisphenol A-Co-Epichlorohydrin) and Poly(Vinyl Ethyl Ether). Polymer 2010, 51 (22), 5151–5164.

(61). Correia DM; Costa CM; Nunes-Pereira J; Silva MM; Botelho G; Ribelles J; Lanceros-Mendez S Physicochemical Properties of Poly(Vinylidene Fluoride-Trifluoroethylene)/Poly(Ethylene Oxide) Blend Membranes for Lithium Ion Battery Applications: Influence of Poly(Ethylene Oxide) Molecular Weight. Solid State Ionics 2014, 268, 54–67.

(62). Ito H; Russell TP; Wignall GD Interactions in Mixtures of Poly(Ethylene Oxide) and Poly(Methyl Methacrylate). Macromolecules 1987, 20 (9), 2213–2220.

(63). Yeh C; Hou T; Chen H; Yeh L; Chiu F-C; Muller AJ; Hadjichristidis N Lower Critical Ordering Transition of Poly(Ethylene Oxide)-Block-Poly(2-Vinylpyridine). Macromolecules 2011, 44, 440–443.

(64). Watanabe M; Hirakimoto T; Mutoh S; Nishimoto A Polymer Electrolytes Derived from Dendritic Polyether Macromonomers. Solid State Ionics 2002, 148 (3–4), 399–404.

(65). Sun B; Mindemark J; Edström K; Brandell D Polycarbonate-Based Solid Polymer Electrolytes for Li-Ion Batteries. Solid State Ionics 2014, 262, 738–742.

(66). Zhang J; Yang J; Dong T; Zhang M; Chai J; Dong S; Wu T; Zhou X; Cui G Aliphatic Polycarbonate-Based Solid-State Polymer Electrolytes for Advanced Lithium Batteries: Advances and Perspective. Small 2018, 14 (36), 1–16.

(67). Pesko DM; Webb MA; Jung Y; Zheng Q; Miller TF; Coates W; Balsara NP Universal Relationship between Conductivity and Solvation-Site Connectivity in Ether-Based Polymer Electrolytes. Macromolecules 2016, 49, 5244–5255.
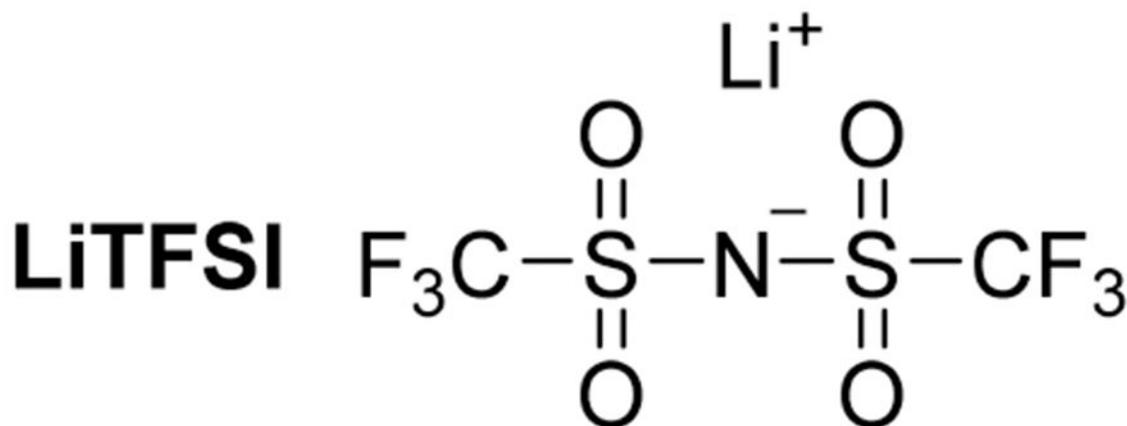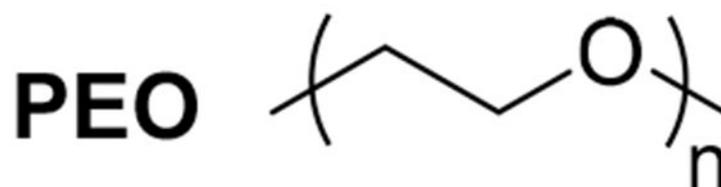
PEO

P(2EO-MO)

LiTFSI

Figure 1.
Chemical structure of poly(ethylene oxide) (PEO), poly(1,3,6-trioxocane) (P(2EO-MO)),
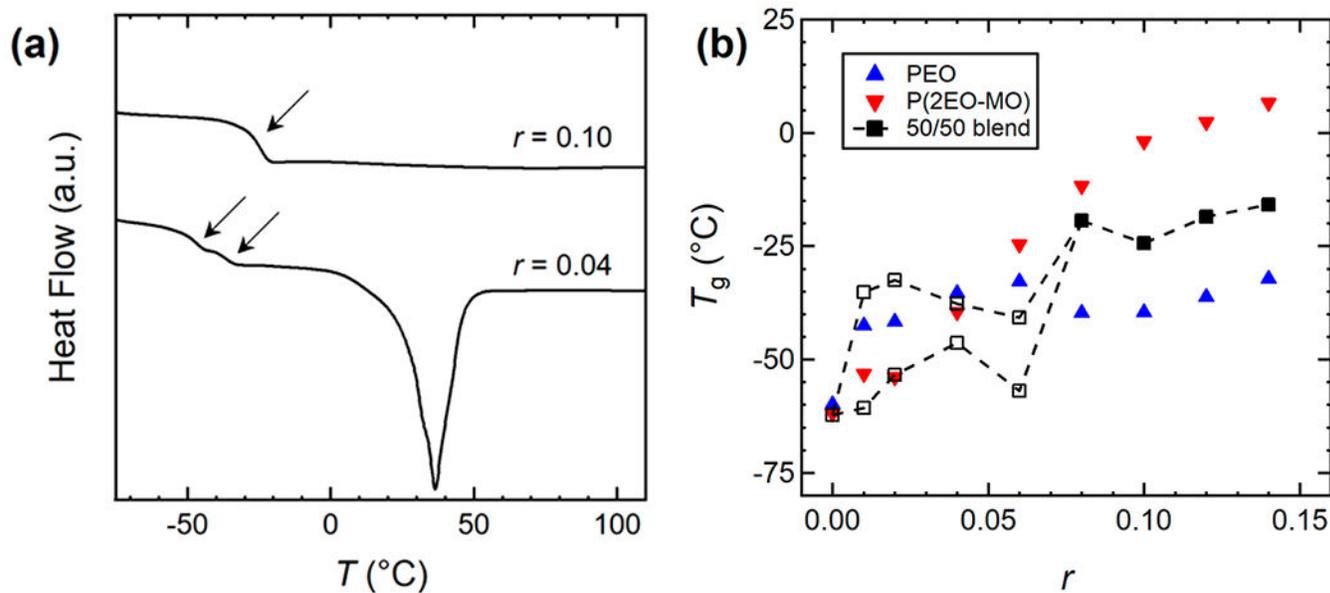and lithium bis(trifluoromethanesulfonyl) imide (LiTFSI).

Figure 2.
(a) Representative DSC curves showing one T_g for a 50/50 blend of PEO (M_n = 35.0 kg mol^{-1}) and P(2EO-MO) (M_n = 26.1 kg mol^{-1}) at $_r$ = 0.10 and two T_g values at r = 0.04. Arrows denote regions associated with the glass transition. (b) T_g as a function of salt concentration, r, for each conventional polymer electrolyte system (solid blue triangles for PEO (M_n = 100 kg mol^{-1}) and solid red triangles for P(2EO-MO) (M_n = 55.2 kg mol^{-1})) and the polymer blend electrolytes. Polymer blends possessing a single T_g at high r values (0.08 r 0.14) and blends exhibiting two T_g values at low r values (0.02 r 0.06) are denoted by closed black squares and open black squares, respectively. The uncertainty of the T_g measurements is assumed to be that of the instrument's given calorimetric reproducibility and precision (±0.05%). Data for PEO and P(2EO-MO) were taken from ref 9.
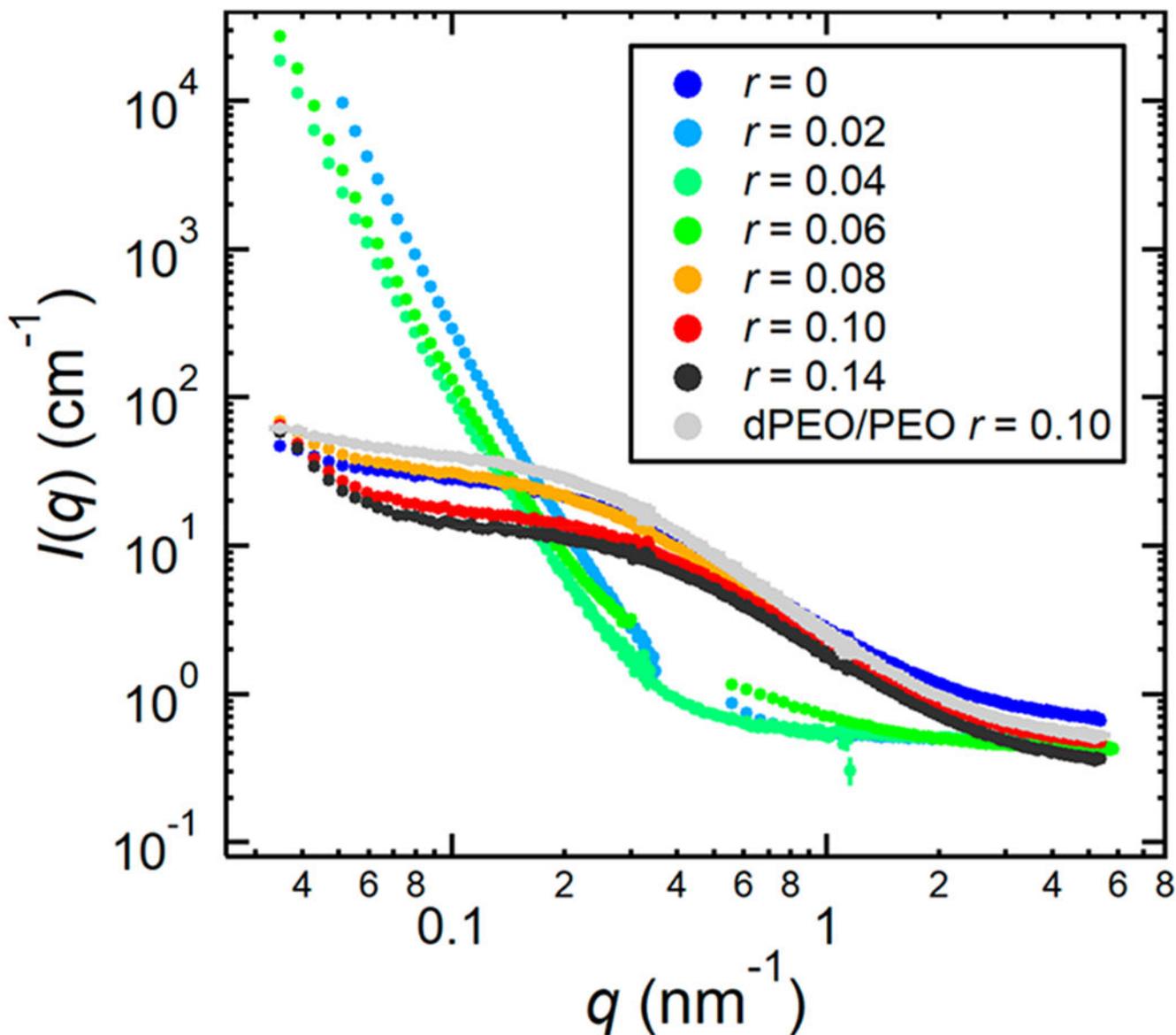
Figure 3.
Measured absolute SANS intensity, $I(q)$, vs scattering vector, q, at 90 °C, for blends of dPEO (M_n = 35.0 kg mol^{-1}) and P(2EO-MO) (M_n = 26.7 kg mol^{-1}) at varying LiTFSI salt concentrations, r, and a dPEO/PEO sample with r = 0.10. Note that for r = 0.02 and r = 0.06 there is an intermediate range of q that was not recorded due to insufficient beamtime. Error bars represent one standard deviation of the scattering data and in most cases are smaller than the data points.
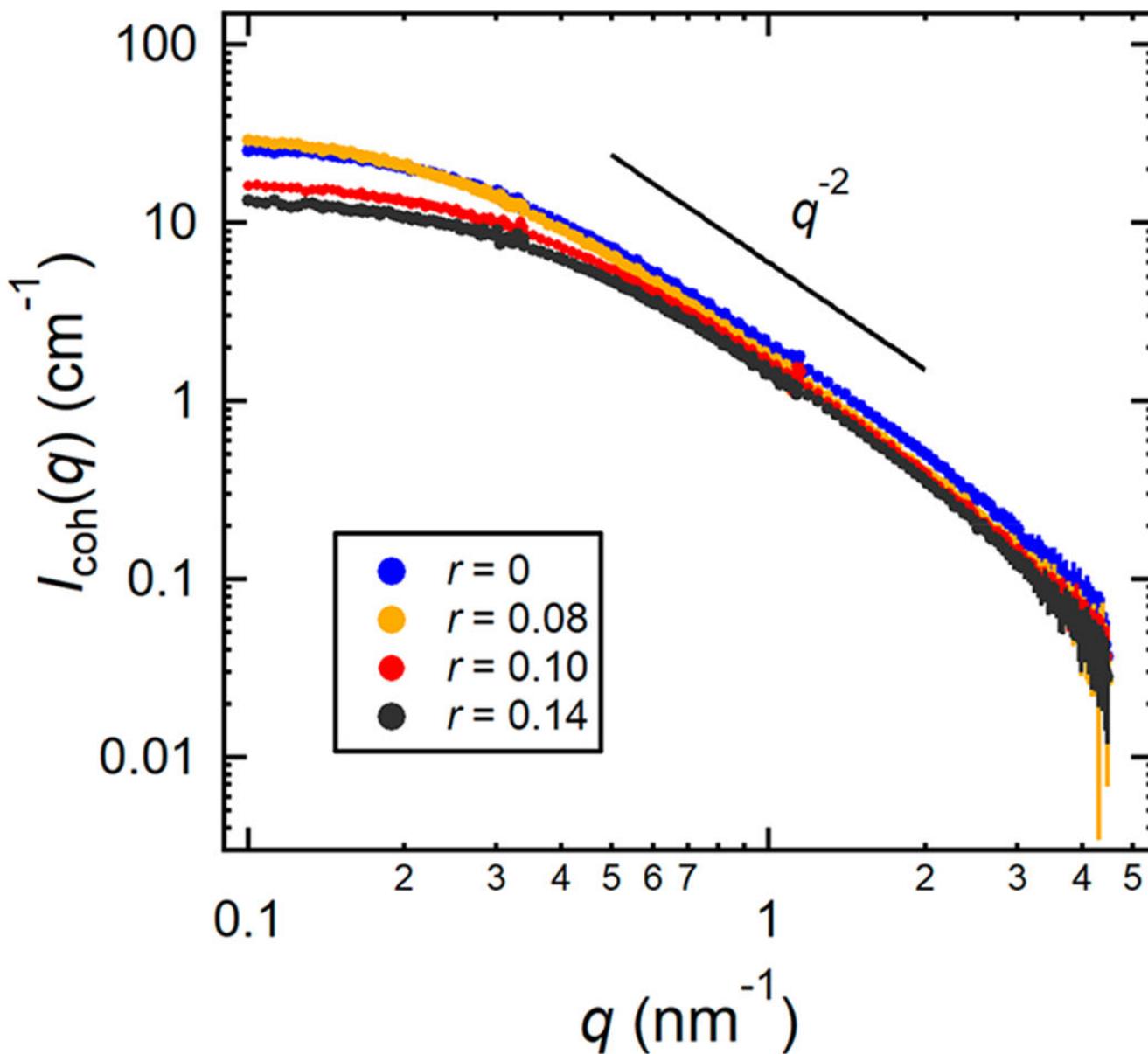
Figure 4.
SANS intensities, $I_{coh}(q)$, plotted as a function of the magnitude of the scattering vector, q, at 90 °C for the dPEO/P(2EOMO)/LiTFSI (P(2EO-MO) M_n = 26.7 kg mol^{-1}) blends at the miscible salt concentrations. Error bars represent one standard deviation of the scattering data and in most cases are smaller than the data points.
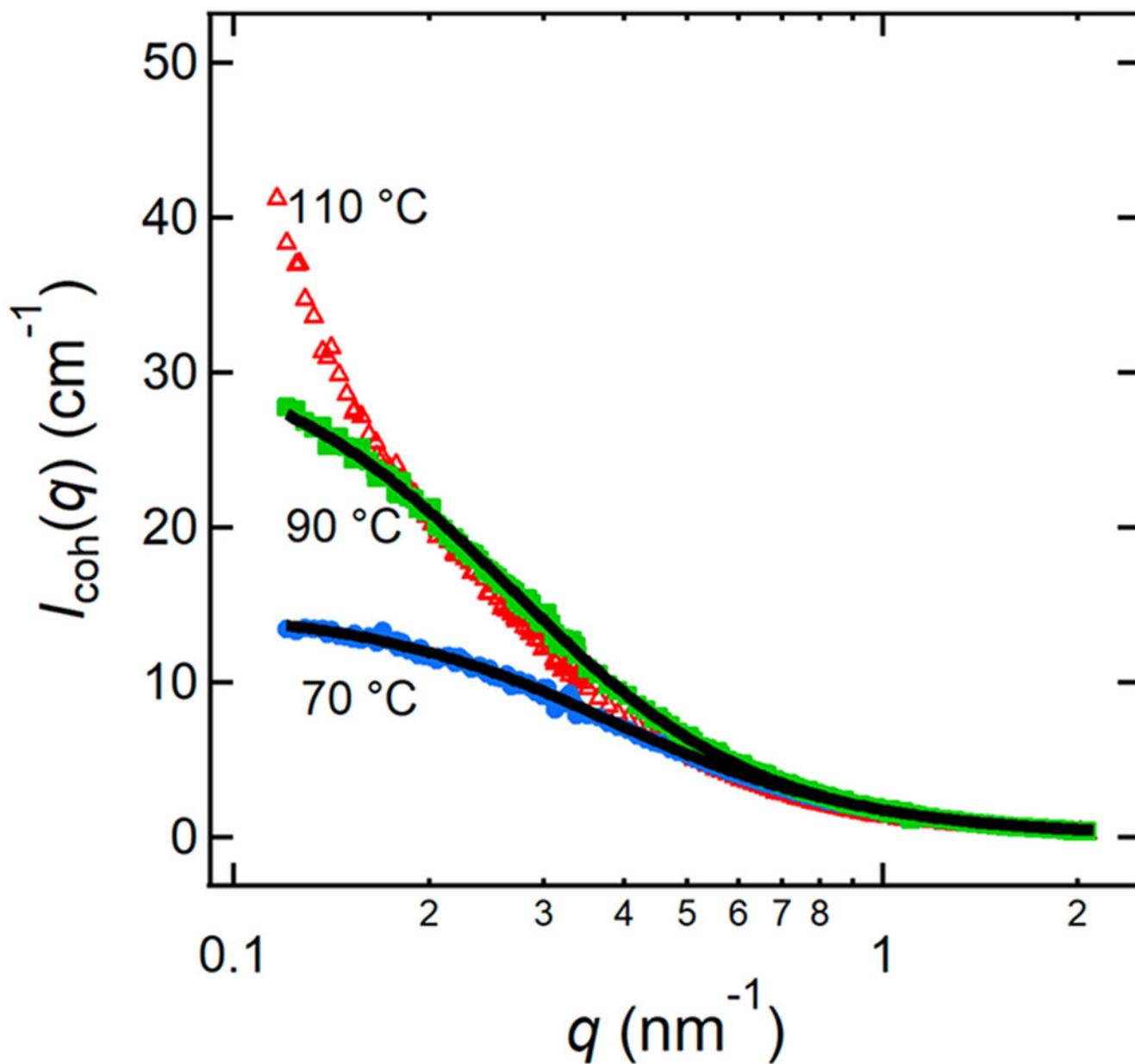
Figure 5.
RPA fits (solid black lines) for a dPEO/P(2EO-MO)/LiTFSI (P(2EO-MO) $M_n = 26.7$ kg mol^{-1}) blend with $r = 0.08$ at 70 °C (filled blue circles) and 90 °C (filled green squares). The 110 °C measurements (open red triangles) indicate phase separation. Error bars represent one standard deviation of the scattering data and in most cases are smaller than the data points.
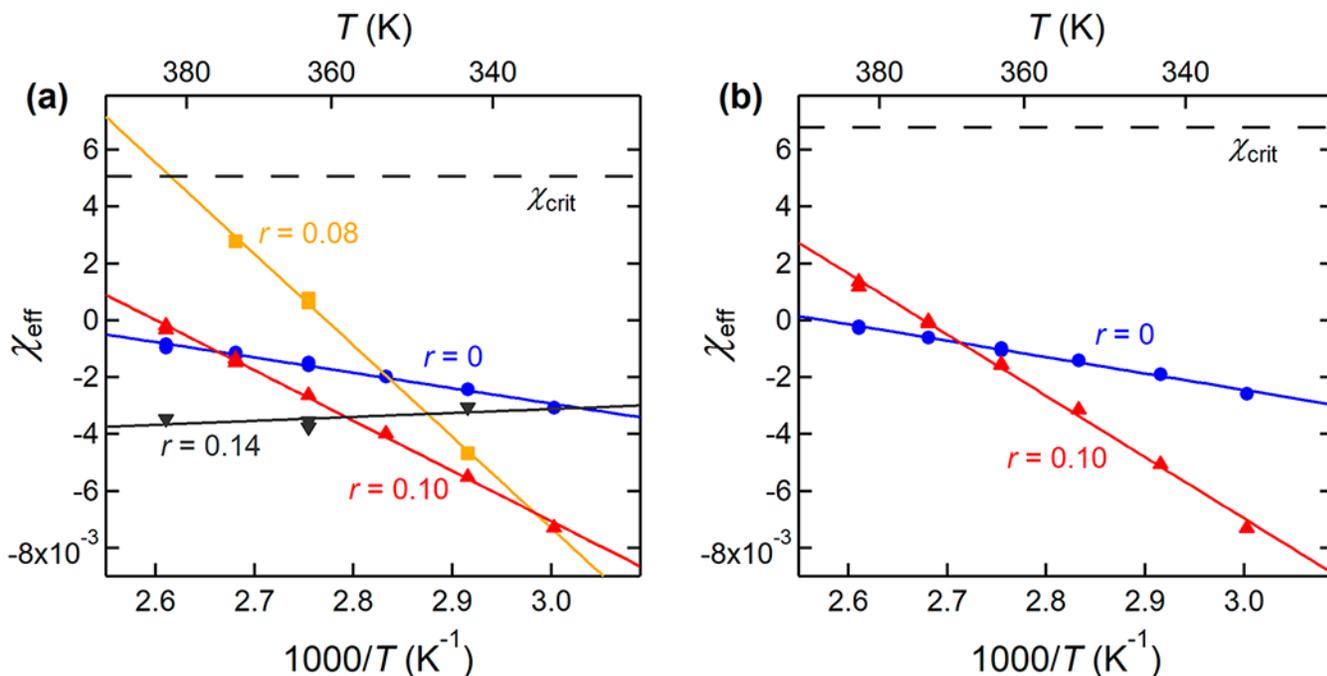
Figure 6.

Effective Flory–Huggins interaction parameter, χ_{eff}, as a function of inverse temperature, $1/T$, for the dPEO/P(2EO-MO)/LiTFSI blend (a) with higher P(2EO-MO) molar mass ($M_n = 26.7$ kg mol^{-1}) and (b) with lower P(2EO-MO) molar mass ($M_n = 16.0$ kg mol^{-1}). The solid lines are linear fits to the data according to eq 16; values for A and B are reported in Table 4. Error bars represent one standard deviation of the χ_{eff} fits and are smaller than the symbols. Typical error bars on χ range between 5 and 20%, as previously shown in ref 24.
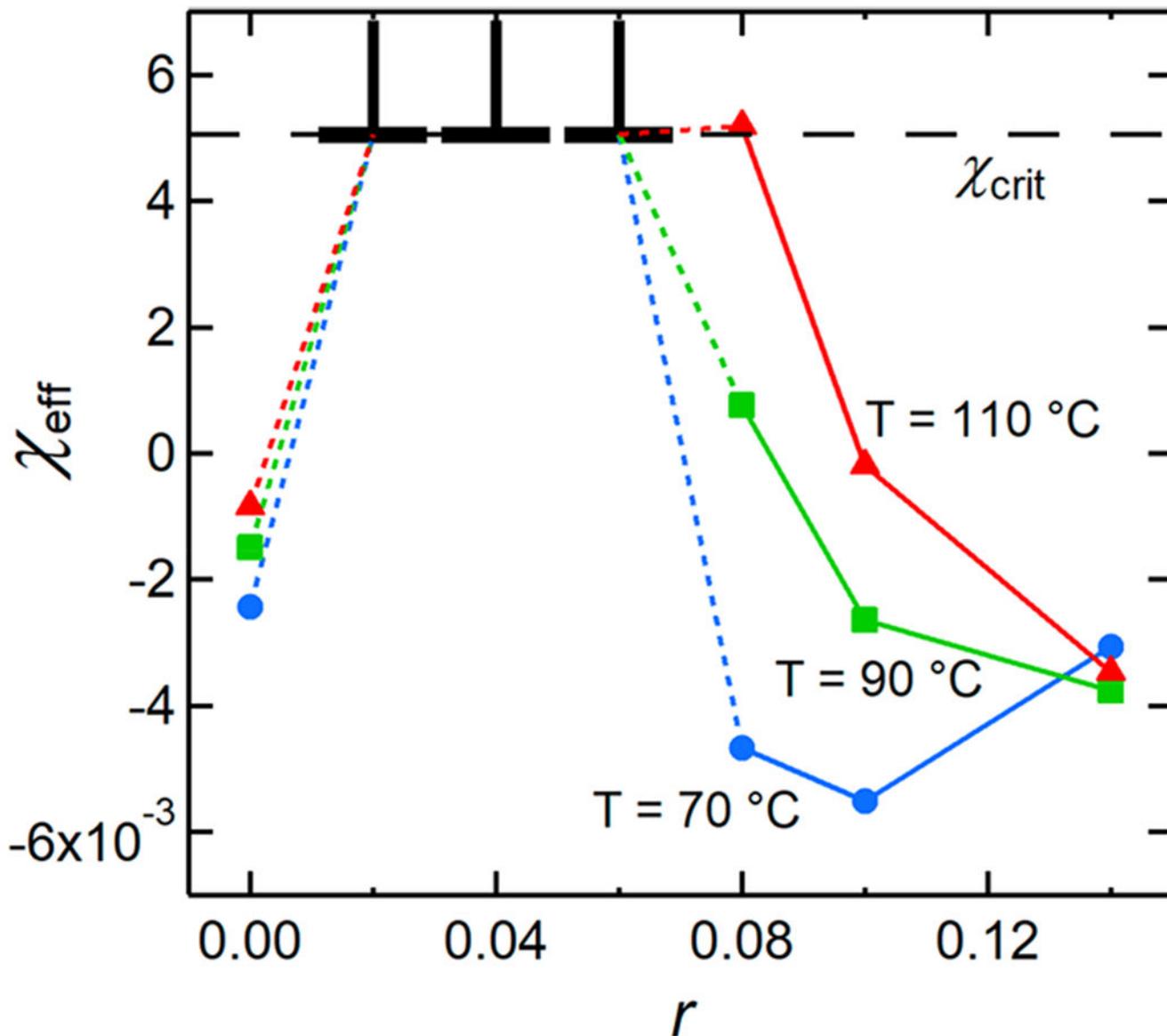
Figure 7.
Effective Flory–Huggins interaction parameter, χ_{eff}, for the dPEO/P(2EO-MO)/LiTFSI (P(2EO-MO) M_n = 26.7 kg mol^{-1}) blends as a function of salt concentration, r, at three different temperatures: 70 °C (blue circles), 90 °C (green squares), and 110 °C (red triangles). The lower limit of the error bars at 0.02 ≤ r ≤ 0.06 is the critical value for the Flory–Huggins interaction parameter, χ_{crit}, at which this system phase separates. Error bars for the solid markers represent one standard deviation of the χ_{eff} fits and are smaller than the symbols.
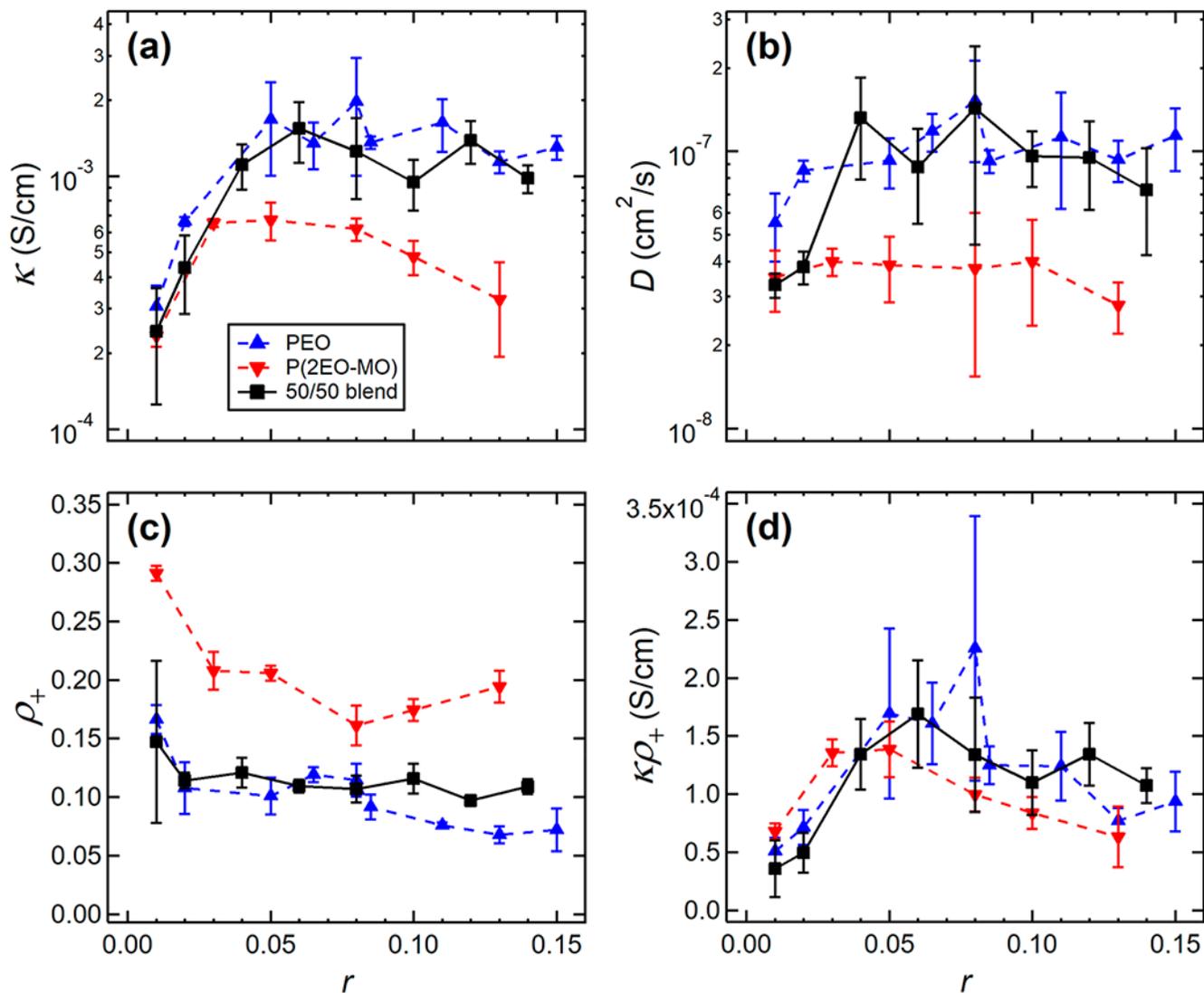
Figure 8.
Electrochemical characterization of the PEO/P(2EO-MO)/LiTFSI blend as a function of salt concentration, r, compared with conventional PEO/LiTFSI ($M_n = 35.0$ kg mol^{-1}) and P(2EO-MO)/LiTFSI ($M_n = 55.2$ kg mol^{-1}) polymer electrolyte systems. (a) Ionic conductivity, κ, from ac impedance spectroscopy of symmetric cells with blocking electrodes. (b) Salt diffusion coefficient, D, from restricted diffusion measurements in a lithium symmetric cell. (c) Current fractions, ρ_+, calculated from the Bruce–Vincent method using a lithium symmetric cell. (d) Efficacy, $\kappa\rho_+$. Data were taken at 90 °C. PEO/LiTFSI data were taken from ref 43. Error bars represent the standard deviation of three measurements.

Table 1.

Molar Masses and Dispersities of Homopolymers Used in This Study

polymer	M_n (kg mol^{-1})	
PEO	35.0	1.08
dPEO	35.0	1.09
P(2EO-MO) sample 1	26.1	1.83
P(2EO-MO) sample 2	26.7	1.66
P(2EO-MO) sample 3	16.0	1.76
P(2EO-MO) sample 4	55.2	1.97

Table 2.

Polymer Components of Blends Used in Each Experiment

experiment	component 1	component 2
DSC and electrochemistry	PEO	P(2EO-MO) sample 1
SANS	dPEO	P(2EO-MO) sample 2
SANS	dPEO	P(2EO-MO) sample 3

Table 3.

Volume Fractions, ϕ_i, and α Values Used in RPA Fits of dPEO/P(2EO-MO)/LiTFSI Blends[a]

r	dPEO/P(2EO-MO)/LiTFSI (dPEO M_n = 35.0 kg mol⁻¹; P(2EO-MO) M_n = 26.7 kg mol⁻¹)				dPEO/P(2EO-MO)/LiTFSI (dPEO M_n = 35.0 kg mol⁻¹; P(2EO-MO) M_n = 16.0 kg mol⁻¹)			
	ϕ_1	ϕ_2	$\phi_{polymer}$	α	ϕ_1	ϕ_2	$\phi_{polymer}$	α
0	0.516	0.484	1	1.274 ± 0.007	0.517	0483	1	1.331 ± 0.044
0.08	0.517	0.483	0.742	1.205 ± 0.014				
0.10	0.518	0.482	0.696	1.173 ± 0.001	0.517	0483	0.705	1.212 ± 0.011
0.14	0.515	0.485	0.621	1.122 ± 0.002				

[a]The errors shown correspond to one standard deviation from the temperature averaging.

Table 4.

A and B Constants for dPEO/P(2EO-MO)/LiTFSI Blends at Various Salt Concentrations, r, and Their Linear Fit R^2 Values[a]

| r | dPEO/P(2EO-MO)/LiTFSI (P(2EO-MO) M_n = 26.7 kg mol^{-1}) | | | dPEO/P(2EO-MO)/LiTFSI (P(2EO-MO) M_n = 16.0 kg mol^{-1}) | | |
	A	B	R^2	A	B	R^2
0	-5.401 ± 0.241	0.0133 ± 0.0007	0.986	-5.773 ± 0.172	0.0149 ± 0.0005	0.994
0.08	-32.127 ± 1.146	0.0891 ± 0.0032	0.997			
0.10	-17.682 ± 0.305	0.0460 ± 0.0008	0.998	-21.537 ± 0.480	0.0576 ± 0.0013	0.997
0.14	1.383 ± 1.350	-0.0072 ± 0.0037	0.344			

[a]The errors shown represent one standard deviation of uncertainty for the fit for A and B according to eq 16.